Acta Crystallographica Section F
Structural Biology and Crystallization Communications
ISSN 1744-3091

Binding of the unreactive substrate analog L-2-amino-3-guanidinopropionic acid (dinor-L-arginine) to human arginase I

Edward L. D'Antonio and David W. Christianson*

Roy and Diana Vagelos Laboratories, Department of Chemistry, University of Pennsylvania, Philadelphia, PA 19104-6323, USA

Correspondence e-mail: chris@sas.upenn.edu

Received 30 May 2012
Accepted 19 June 2012

PDB References: Mn_2^{2+}-HAI–AGPA complex, 4fci; Co_2^{2+}-HAI–AGPA complex, 4fck.

Human arginase I (HAI) is a binuclear manganese metalloenzyme that catalyzes the hydrolysis of L-arginine to form L-ornithine and urea through a metal-activated hydroxide mechanism. Since HAI regulates L-Arg bioavailability for NO biosynthesis, it is a potential drug target for the treatment of cardiovascular diseases such as atherosclerosis. X-ray crystal structures are now reported of the complexes of Mn_2^{2+}-HAI and Co_2^{2+}-HAI with L-2-amino-3-guanidinopropionic acid (AGPA; also known as dinor-L-arginine), an amino acid bearing a guanidinium side chain two methylene groups shorter than that of L-arginine. Hydrogen bonds to the α-carboxylate and α-amino groups of AGPA dominate enzyme–inhibitor recognition; the guanidinium group does not interact directly with the metal ions.

1. Introduction

Arginase is a hydrolytic metalloenzyme that is responsible for the conversion of the substrate L-arginine into the products L-ornithine and urea (Fig. 1; Christianson, 2005). A binuclear manganese cluster is required for catalysis through a metal-activated hydroxide mechanism. Two human arginase isozymes, designated type I and type II, are related by 60% amino-acid sequence identity and both isozymes have yielded X-ray crystal structures (Di Costanzo *et al.*, 2005; Cama *et al.*, 2003). Both isozymes exist as homotrimers in solution and in the crystal.

In recent years, the arginases have been increasingly implicated as potential drug targets in a variety of diseases, such as asthma and pulmonary arterial hypertension (Benson *et al.*, 2011). Upregulated arginase activity results in the degradation of cellular concentrations of L-arginine that would otherwise be utilized by nitric oxide synthase for the regulation of NO-dependent processes such as smooth-muscle relaxation in the airway or vasculature. The attenuation of excessive arginase activity with inhibitors *in vivo* sustains L-arginine concentrations for utilization by nitric oxide synthase.

Modified amino-acid analogs of L-arginine have been studied as alternative substrates of rat arginase I (Reczkowski & Ash, 1994) and *Bacillus caldovelox* arginase (Patchett *et al.*, 1991). These studies demonstrate that the length of the guanidinium side chain is critical for optimal enzyme activity. Owing to the three-dimensional arrangement of the nucleophilic metal-bridging hydroxide ion and the residues responsible for the molecular recognition of the α-carboxylate and α-amino groups of the L-amino acid (Shishova *et al.*, 2009), the longer L-arginine analog L-homoarginine (Fig. 1) is a poor substrate that is hydrolyzed with $\sim 10^3$-fold reduced catalytic efficiency ($k_{cat}/K_m = 2.8 \times 10^3\ M^{-1}\ s^{-1}$) compared with L-Arg ($k_{cat}/K_m = 2.6 \times 10^6\ M^{-1}\ s^{-1}$) when assayed against rat arginase I (Reczkowski & Ash, 1994). Moreover, given that substrate K_m values are 1.0 and 7.2 mM for L-Arg and L-homoarginine, respectively (Reczkowski & Ash, 1994), it is interesting to note that an L-amino acid with a side chain longer than that of L-arginine binds more weakly in the active site, insofar that the K_m values reflect enzyme–substrate affinity.

To date, an L-amino acid with a side chain shorter than that of L-arginine has not been evaluated as a potential arginase substrate.

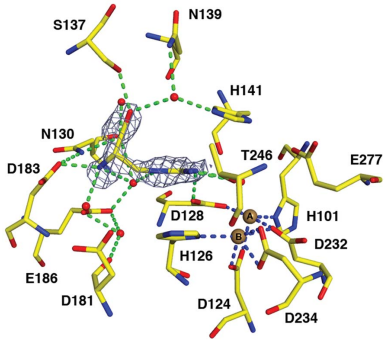

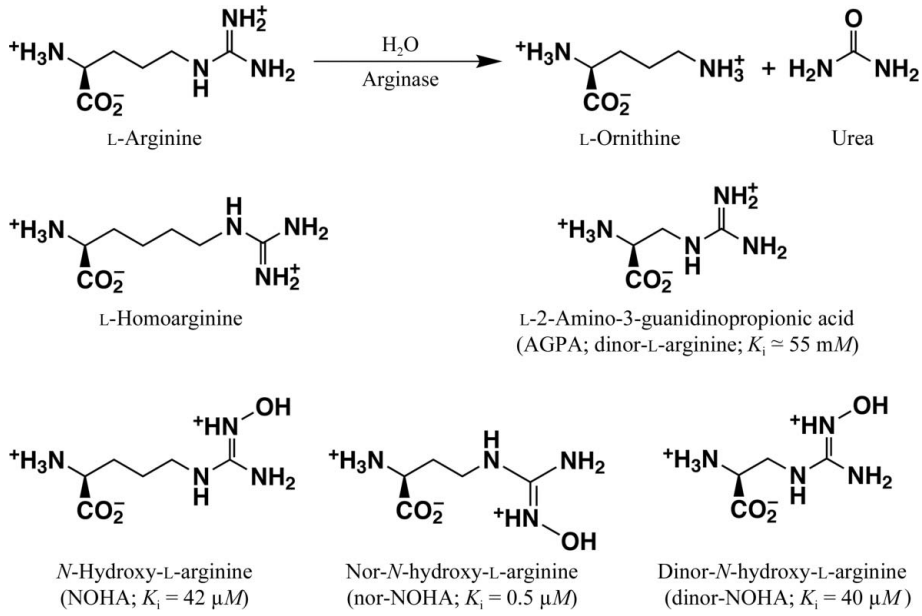

Figure 1
Arginase catalyzes the hydrolysis of L-arginine to form L-ornithine and urea. Extending the L-arginine side chain by one methylene group yields the slowly hydrolyzed substrate L-homoarginine; shortening the L-arginine side chain by two methylene groups yields the poor inhibitor L-2-amino-3-guanidinopropionic acid (AGPA; also known as dinor-L-arginine). Hydroxylation of the guanidinium group of L-arginine and analogs with shorter side chains yields the inhibitors NOHA, nor-NOHA and dinor-NOHA.

However, derivatives of L-arginine with shorter side chains have been studied as inhibitors (Fig. 1). For example, consider L-arginine derivatized with a hydroxylated guanidinium group, *N*-hydroxy-L-arginine (NOHA), which inhibits rat liver arginase with a K_i value of 42 μ*M* (Daghigh *et al.*, 1994). Derivatives of this amino acid with side chains that are one methylene group shorter (nor-NOHA) or two methylene groups shorter (dinor-NOHA) inhibit rat liver arginase with K_i values of 0.5 and 40 μ*M*, respectively (Custot *et al.*, 1997; Moali *et al.*, 2000). Thus, the active site of arginase can be somewhat promiscuous in accommodating shorter side chains in L-arginine-based guanidinium derivatives; can arginase accommodate a shorter side chain in a potential L-arginine-based substrate bearing an intact guanidinium group?

The L-arginine analog L-2-amino-3-guanidinopropionic acid (AGPA; also known as dinor-L-arginine; see Fig. 1) has a guanidinium side chain that is two methylene groups shorter than that of L-arginine. We now report that AGPA is not a substrate but instead is a weak inhibitor of human arginase I (HAI). A previous report showed that AGPA is also a weak inhibitor of *B. caldovelox* arginase (Patchett *et al.*, 1991). To understand why AGPA is not an arginase substrate and to understand the molecular basis for its weak inhibitory activity, we report the X-ray crystal structures of Mn_2^{2+}-HAI and Co_2^{2+}-HAI complexed with AGPA. While Mn_2^{2+}-HAI is the native form of arginase as it functions *in vivo*, Co_2^{2+}-HAI is said to be 11-fold more active than Mn_2^{2+}-HAI and is being explored as a potential cancer treatment targeting tumor cells auxotrophic for L-arginine (Stone *et al.*, 2010; Glazer *et al.*, 2011; Mauldin *et al.*, 2012). Accordingly, structure–function comparisons of ligand binding to Mn_2^{2+}-HAI and Co_2^{2+}-HAI may inform the consideration of Co_2^{2+}-HAI as a potential protein drug (D'Antonio & Christianson, 2011).

2. Materials and methods

2.1. Chemicals

L-2-Amino-3-guanidinopropionic acid hydrochloride (AGPA) was purchased from Sigma and used without further purification.

2.2. Preparation of the crystalline AGPA complexes

Recombinant HAI was expressed and purified as described by Di Costanzo *et al.* (2005). Crystals of unliganded Mn_2^{2+}-HAI were prepared as described previously (Di Costanzo *et al.*, 2007), followed by soaking one of these crystals in 50 m*M* AGPA, 5 m*M* $MnCl_2$, 100 m*M* bicine pH 8.5, 32%(*v*/*v*) Jeffamine ED-2001 for 21 h to yield the Mn_2^{2+}-HAI–AGPA complex. The Co_2^{2+}-HAI–AGPA complex was prepared by soaking a Co_2^{2+}-HAI crystal (D'Antonio & Christianson, 2011) in 20 m*M* AGPA, 5 m*M* $CoCl_2$, 100 m*M* bicine pH 8.5, 32%(*v*/*v*) Jeffamine ED-2001 for 18 h. Crystals were flash-cooled in liquid nitrogen, with the mother liquor of their corresponding soaking solutions serving as the cryoprotectant.

2.3. Data collection and structure determination

X-ray diffraction data were collected on beamline X29 at the National Synchrotron Light Source, Brookhaven National Laboratory, Upton, New York, USA from single crystals of the Mn_2^{2+}-HAI–AGPA complex (λ = 1.0750 Å) and the Co_2^{2+}-HAI–AGPA complex (λ = 0.9795 Å). Diffraction data were indexed, integrated and scaled using the *HKL*-2000 suite (Otwinowski & Minor, 1997). The crystals were isomorphous with those obtained for the Mn_2^{2+}-HAI–ABH complex (Di Costanzo *et al.*, 2005) and similarly exhibited hemihedral twinning. Data-collection statistics are reported in Table 1.

The structures were solved by molecular replacement with the program *Phaser* (McCoy *et al.*, 2005) as implemented in *CCP*4 (Winn *et al.*, 2011), using the atomic coordinates of chain *A* of the Mn_2^{2+}-HAI–ABH complex (PDB entry 2aeb; Di Costanzo *et al.*, 2005) less inhibitor, Mn^{2+} ions and solvent atoms as the search probe for rotation-function and translation-function calculations. Each refinement was performed with *CNS* (v.1.2; Brünger *et al.*, 1998) and model building was performed with *Coot* (v.0.6.1; Emsley & Cowtan, 2004). The hemihedral twinning-operation parameters used in refinement were $-h$, $-k$ and l; the twinning fraction was 0.44 (Table 1).

Crystallographic refinement of each structure against twinned intensity data was performed as described previously (Di Costanzo *et*

al., 2005). Water molecules were included in the later stages of each refinement. For the Mn_2^{2+}-HAI–AGPA complex a gradient OMIT map showed AGPA bound only in monomer *A*; however, gradient OMIT maps for the Co_2^{2+}-HAI–AGPA complex clearly showed ligands bound to the active sites of both monomers in the asymmetric unit, and ligand atoms were added and refined with full occupancy. The disordered segments Met1–Ser5 and Pro320–Lys322 at the N- and C-termini, respectively, were excluded from all final models. Ramachandran plots showed that Gln65 adopted a disallowed conformation in monomer *A* of each structure. Generally speaking, Gln65 was characterized by well defined electron density in these structures, so its conformation was not ambiguous. Moreover, this residue adopted a similar conformation in Mn_2^{2+}-HAI (PDB entry 2pha; Di Costanzo *et al.*, 2007), so its unfavorable conformation was not judged to be an artifact. Data-collection and refinement statistics for all structure determinations are recorded in Table 1.

Table 1
Data-collection and refinement statistics.

Values in parentheses are for the highest resolution shell.

	Mn_2^{2+}-HAI–AGPA	Co_2^{2+}-HAI–AGPA
Data collection		
Resolution limits (Å)	50.0–1.82	50.0–1.90
Total/unique reflections measured	274027/57670	226674/49901
Space group	*P*3	*P*3
Unit-cell parameters	$a = b = 90.85$, $c = 69.77$, $\alpha = \beta = 90$, $\gamma = 120$	$a = b = 90.45$, $c = 69.36$, $\alpha = \beta = 90$, $\gamma = 120$
R_{merge}†	0.089 (0.183)	0.083 (0.593)
$\langle I/\sigma(I)\rangle$	18.06 (9.31)	17.90 (2.69)
Completeness (%)	99.8 (100)	99.9 (99.2)
Refinement		
Reflections used in refinement	57506	45756
Reflections used in test set	2827	2362
Twinning fraction	0.44	0.44
R_{twin}‡	0.142	0.133
$R_{twin,free}$§	0.189	0.184
Water molecules¶	254	238
Ligand molecules¶	1	2
Metal ions¶	4	4
Root-mean-square deviations††		
Bonds (Å)	0.007	0.007
Angles (°)	1.6	1.5
Ramachandran plot†† (%)		
Allowed	89.8	87.8
Additionally allowed	9.8	11.6
Generously allowed	0.2	0.4
Disallowed	0.2	0.2
PDB code	4fci	4fck

† $R_{merge} = \sum_{hkl}\sum_i |I_i(hkl) - \langle I(hkl)\rangle| / \sum_{hkl}\sum_i I_i(hkl)$, where $I_i(hkl)$ is the observed intensity and $\langle I(hkl)\rangle$ is the average intensity calculated from replicate data. ‡ $R_{twin} = \sum_{hkl} ||F_{obs}| - |F_{calc}|| / \sum_{hkl} |F_{obs}|$ for reflections contained in the working set. $|F_o|$ and $|F_c|$ are the observed and calculated structure-factor amplitudes, respectively. § $R_{twin,free} = \sum_{hkl} ||F_{obs}| - |F_{calc}|| / \sum_{hkl} |F_{obs}|$ for 5% of reflections contained in the test set held aside during refinement. ¶ Per asymmetric unit. †† Calculated using *PROCHECK* (Laskowski *et al.*, 1993).

3. Results and discussion

AGPA is a weak inhibitor of HAI, with a K_i value of approximately 55 m*M* (data not shown). This inhibition constant is consistent with the relatively poor inhibition of *B. caldovelox* arginase previously observed for AGPA, although no inhibition constant was reported against this enzyme (Patchett *et al.*, 1991). For reference, the K_i value of the inert amino acid L-valine is 3.6 m*M* against rat mammary gland arginase (Fuentes *et al.*, 1994), so the weak inhibitory activity observed for AGPA against HAI suggests that the short guanidinium side chain does not make any favorable interactions with the enzyme active site. We confirmed that AGPA does not undergo HAI-catalyzed hydrolysis using a colorimetric assay for the detection of urea, which reacts with α-isonitrosopropiophenone to generate a chromophore absorbing at 550 nm (Archibald, 1945). No chromophore production was observed and hence no urea hydrolysis product was generated after incubating 0.34 µ*M* HAI and 20 m*M* AGPA for 20 min at room temperature (data not shown).

Despite the weak affinity of AGPA for binding to HAI, we successfully prepared crystals of AGPA complexes of Mn_2^{2+}-HAI and Co_2^{2+}-HAI. The overall protein structure in the Mn_2^{2+}-HAI–AGPA complex is very similar to that of unliganded Mn_2^{2+}-HAI (PDB entry 2zav; Di Costanzo *et al.*, 2007), with an r.m.s. deviation of 0.21 Å for 312 C^α atoms. Likewise, the overall protein structure in the Co_2^{2+}-HAI–AGPA complex is very similar to that of unliganded Co_2^{2+}-HAI (PDB entry 3the; D'Antonio & Christianson, 2011), with an r.m.s. deviation of 0.49 Å for 314 C^α atoms. Therefore, binding of AGPA does not cause any significant tertiary-structural or quaternary-structural changes. The overall protein structures in the Mn_2^{2+}-HAI–AGPA and Co_2^{2+}-HAI–AGPA complexes are essentially identical, with an r.m.s. deviation of 0.18 Å for 312 C^α atoms. As expected based on the lack of any observable hydrolytic activity towards AGPA, the guanidinium moiety of AGPA is intact in each complex, as revealed in the electron-density maps in Fig. 2.

The α-carboxylate and α-amino groups of AGPA make numerous hydrogen-bond interactions in the enzyme active site. Specifically, the α-amino group accepts hydrogen bonds from the side chain of Asp183 and two water molecules. Interestingly, one of these water molecules also accepts a hydrogen bond from the side chain N^γ—H group of AGPA. The α-carboxylate group accepts hydrogen bonds from the side chains of Asn130 and Ser137 and three water molecules. Water molecules that interact with the α-carboxylate and α-amino groups of AGPA make hydrogen-bond interactions with protein residues, as indicated in Figs. 2(*a*) and 2(*b*). All of the hydrogen-bond interactions between protein residues and the α-carboxylate and α-amino groups of AGPA, whether direct or water-mediated, are generally observed for the binding of other amino-acid inhibitors to HAI (Di Costanzo *et al.*, 2005). Recent mutagenesis studies with rat liver arginase indicate that hydrogen-bond interactions with the α-carboxylate and α-amino groups of L-arginine dominate the molecular recognition of the substrate (Shishova *et al.*, 2009), so it is reasonable to expect that such interactions dominate the molecular recognition of AGPA in the active site of HAI.

With the α-carboxylate and α-amino groups of AGPA anchored in the outer active-site cleft of Mn_2^{2+}-HAI and Co_2^{2+}-HAI in a nearly identical fashion, the electrophilic C atom of the AGPA guanidinium group is held somewhat distant (∼5 Å) from the active-site metal ions. Therefore, a nucleophilic metal-bound hydroxide ion would not be able to attack the guanidinium group of AGPA. This structural feature in each AGPA complex accounts for the complete lack of any observable catalytic activity against AGPA. However, it is curious that AGPA binding appears to trigger some changes in the metal-coordination polyhedra. While the Mn^{2+}–Mn^{2+} separation remains constant at 3.3 Å in unliganded Mn_2^{2+}-HAI and the Mn_2^{2+}-HAI–AGPA complex, the Co^{2+}–Co^{2+} separation decreases from 3.4 Å in unliganded Co_2^{2+}-HAI to 3.2 Å in the Co_2^{2+}-HAI–AGPA complex. While it could be argued that these differences lie within the average coordinate error of the crystal structure determinations, the positions of electron-rich metal ions are more accurately determined in protein crystal structures; hence, differences in metal-ion separations may not be artifactual. Additionally, no ordered metal-bound solvent molecules are observed in the structure of the Mn_2^{2+}-HAI–AGPA complex; a single Co_A^{2+}-bound water molecule is observed in the Co_2^{2+}-HAI–

AGPA complex and this water molecule donates a hydrogen bond to the carboxylate of Asp128 and accepts a hydrogen bond from the N^{ε}—H group of AGPA. Intriguingly, both complexes lack electron density corresponding to an ordered metal-bridging hydroxide ion, except for in monomer *B* of the Co_2^{2+}-HAI–AGPA complex. With the positively charged guanidinium group of AGPA anchored ∼5 Å away from the metal ions, it is possible that the resultant electrostatic interaction with the negatively charged metal-bridging hydroxide ion results in some disorder of the hydroxide ion, resulting in weak or unobserved electron density.

The guanidinium group of AGPA accepts hydrogen bonds from the carboxylate side chain of Asp128 (Figs. 2*a* and 2*b*) and accepts a hydrogen bond from the Co_A^{2+}-bound water molecule in the Co_2^{2+}-HAI-AGPA complex (Fig. 2*b*). However, since the inhibitory potency of AGPA is no better than that measured for the inert amino-acid inhibitor L-valine (Fuentes *et al.*, 1994), these interactions do not

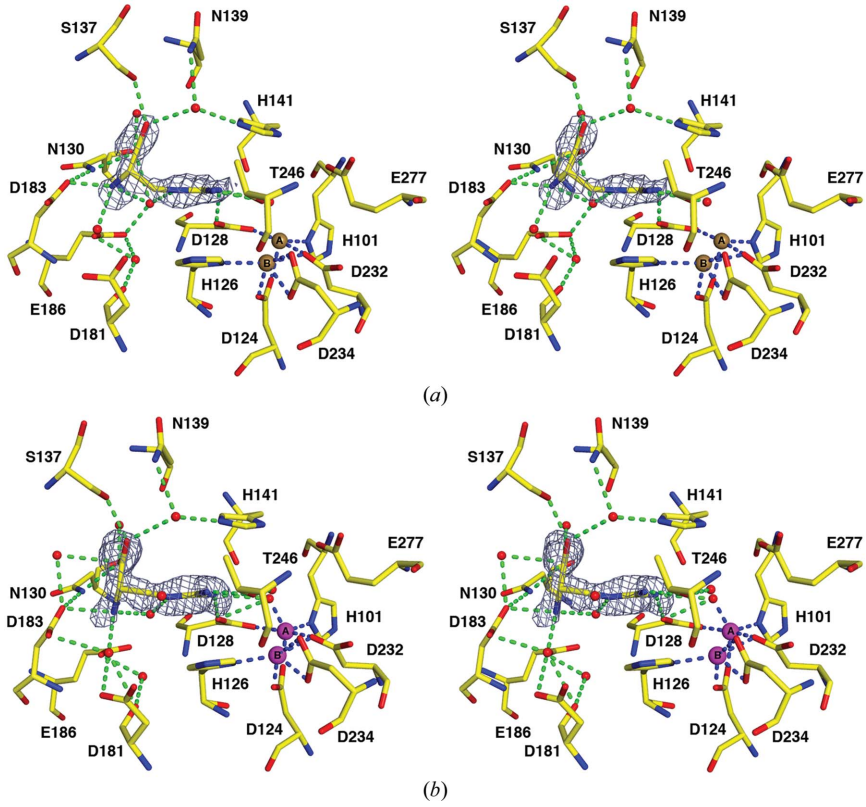

Figure 2
(*a*) OMIT map of AGPA bound in the active site of Mn_2^{2+}-HAI contoured at 3.0σ. Atoms are color-coded as follows: C, yellow; N, blue; O, red. Mn^{2+} ions appear as brown spheres and solvent molecules are shown as red spheres. Metal-coordination and hydrogen-bond interactions are represented by blue and green dashed lines, respectively. (*b*) Simulated-annealing OMIT map of AGPA bound in the active site of Co_2^{2+}-HAI contoured at 3.3σ. Atoms and intermolecular interactions are color-coded as in (*a*) except that Co^{2+} ions appear as magenta spheres.

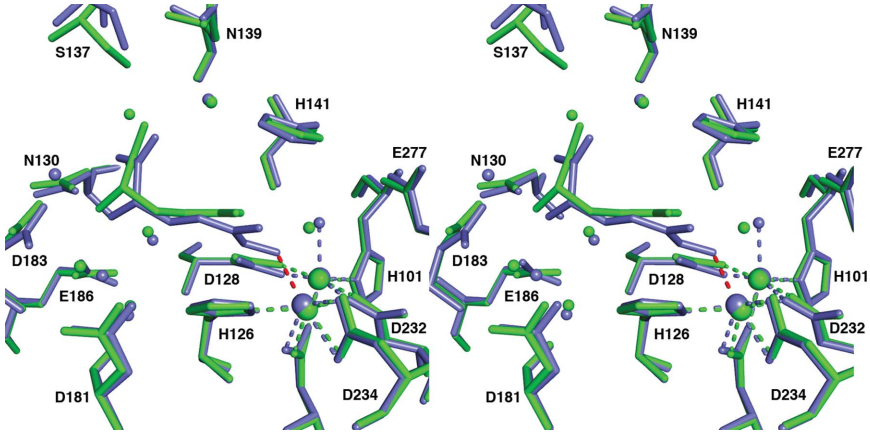

Figure 3
Superposition of the Mn_2^{2+}-HAI–AGPA complex (all atoms and interactions are color-coded green) and the Mn_2^{2+}-rat arginase I–dinor-NOHA complex (PDB entry 1t4t; Cama *et al.*, 2004; all atoms and interactions are color-coded blue). In order for the *N*-hydroxy moiety of dinor-NOHA to achieve metal coordination (red dashed line), the amino acid must shift ∼0.5 Å towards the metal cluster relative to the binding position of AGPA. While this results in some lengthening of the hydrogen-bond interactions wtih the α-carboxylate and α-amino groups of dinor-NOHA, the inhibitory potency of dinor-NOHA is more than 10^3-fold greater than that of AGPA.

appear to make a significant contribution to enzyme–inhibitor affinity. Strikingly, hydroxylation of the guanidinium group of AGPA yields dinor-NOHA (Fig. 1), which exhibits a more than 10^3-fold greater inhibitory potency (Moali *et al.*, 2000). The X-ray crystal structure of rat arginase I complexed with dinor-NOHA revealed that the hydroxyl group coordinates to the Mn_B^{2+} ion (Cama *et al.*, 2004). As such, dinor-NOHA represents the minimum length required for an amino-acid inhibitor of arginase. An ideal arginase inhibitor is one bearing α-carboxylate and α-amino groups that can interact with the amino-acid recognition motif and a side chain that can make a strong coordination interaction with one or both of the active-site metal ions. The side chain of AGPA is too short to realise this ideal, whereas that of dinor-NOHA achieves this minimum (Fig. 3), thereby contributing to enhanced inhibitory potency.

4. Conclusions

The ability of L-arginine derivatives to undergo catalysis or to inhibit arginase depends on the length of the amino-acid side chain. Although L-homoarginine (*i.e.* L-arginine with a side chain one methylene group longer) is a slowly hydrolyzed substrate of arginase, no catalytic activity whatsoever is observed for AGPA (*i.e.* L-arginine with a side chain two methylene groups shorter). Unfortunately, the analog of L-arginine that is only one methylene group shorter than L-arginine (nor-L-arginine) is not available for study; nevertheless, the arginase active site has clearly evolved with optimal specificity for catalysis with L-arginine. The crystal structures of the Mn_2^{2+}-HAI–AGPA and Co_2^{2+}-HAI–AGPA complexes reveal the structural basis for the lack of catalytic activity with AGPA: the amino-acid side chain is too short to allow the guanidinium group to interact with the binuclear metal cluster, while the α-carboxylate and α-amino groups are anchored by the amino-acid recognition motif in the active site.

The inhibitory potency of AGPA is very weak compared with other guanidinium-based amino-acid inhibitors such as NOHA, nor-NOHA and dinor-NOHA (Daghigh *et al.*, 1994; Custot *et al.*, 1997; Moali *et al.*, 2000). It is particularly interesting to compare dinor-NOHA with AGPA, since hydroxylation of the guanidinium group of AGPA yields dinor-NOHA. Our structural comparisons show that dinor-NOHA has the minimum length (but not the ideal length, in view of the higher affinity of nor-NOHA) required for an amino-acid inhibitor to bridge the two affinity determinants in the active site of HAI, and the hydroxylation of the guanidinium group of AGPA accordingly confers more than a 10^3-fold enhancement of inhibitory potency.

This work was supported by National Institutes of Health grant GM49758.

References

Archibald, R. M. (1945). *J. Biol. Chem.* **157**, 507–518.
Benson, R. C., Hardy, K. A. & Morris, C. R. (2011). *J. Allergy*, **2011**, Article ID 736319.
Brünger, A. T., Adams, P. D., Clore, G. M., DeLano, W. L., Gros, P., Grosse-Kunstleve, R. W., Jiang, J.-S., Kuszewski, J., Nilges, M., Pannu, N. S., Read, R. J., Rice, L. M., Simonson, T. & Warren, G. L. (1998). *Acta Cryst.* D**54**, 905–921.
Cama, E., Colleluori, D. M., Emig, F. A., Shin, H., Kim, S. W., Kim, N. N., Traish, A. M., Ash, D. E. & Christianson, D. W. (2003). *Biochemistry*, **42**, 8445–8451.
Cama, E., Pethe, S., Boucher, J.-L., Han, S., Emig, F. A., Ash, D. E., Viola, R. E., Mansuy, D. & Christianson, D. W. (2004). *Biochemistry*, **43**, 8987–8999.
Christianson, D. W. (2005). *Acc. Chem. Res.* **38**, 191–201.
Custot, J., Moali, C., Brollo, M., Boucher, J.-L., Delaforge, M., Mansuy, D., Tenu, J. P. & Zimmermann, J. L. (1997). *J. Am. Chem. Soc.* **119**, 4086–4087.
Daghigh, F., Fukuto, J. M. & Ash, D. E. (1994). *Biochem. Biophys. Res. Commun.* **202**, 174–180.
D'Antonio, E. L. & Christianson, D. W. (2011). *Biochemistry*, **50**, 8018–8027.
Di Costanzo, L., Pique, M. E. & Christianson, D. W. (2007). *J. Am. Chem. Soc.* **129**, 6388–6389.
Di Costanzo, L., Sabio, G., Mora, A., Rodriguez, P. C., Ochoa, A. C., Centeno, F. & Christianson, D. W. (2005). *Proc. Natl Acad. Sci. USA*, **102**, 13058–13063.
Emsley, P. & Cowtan, K. (2004). *Acta Cryst.* D**60**, 2126–2132.
Fuentes, J. M., Campo, M. L. & Soler, G. (1994). *Arch. Int. Physiol. Biochim. Biophys.* **102**, 255–258.
Glazer, E. S., Stone, E. M., Zhu, C., Massey, K. L., Hamir, A. N. & Curley, S. A. (2011). *Transl. Oncol.* **4**, 138–146.
Laskowski, R. A., MacArthur, M. W., Moss, D. S. & Thornton, J. M. (1993). *J. Appl. Cryst.* **26**, 283–291.
Mauldin, J. P., Zeinali, I., Kleypas, K., Woo, J. H., Blackwood, R. S., Jo, C.-H., Stone, E. M., Georgiou, G. & Frankel, A. E. (2012). *Transl. Oncol.* **5**, 26–31.
McCoy, A. J., Grosse-Kunstleve, R. W., Storoni, L. C. & Read, R. J. (2005). *Acta Cryst.* D**61**, 458–464.
Moali, C., Brollo, M., Custot, J., Sari, M. A., Boucher, J.-L., Stuehr, D. J. & Mansuy, D. (2000). *Biochemistry*, **39**, 8208–8218.
Otwinowski, Z. & Minor, W. (1997). *Methods Enzymol.* **276**, 307–326.
Patchett, M. L., Daniel, R. M. & Morgan, H. W. (1991). *Biochim. Biophys. Acta*, **1077**, 291–298.
Reczkowski, R. S. & Ash, D. E. (1994). *Arch. Biochem. Biophys.* **312**, 31–37.
Shishova, E. Y., Di Costanzo, L., Emig, F. A., Ash, D. E. & Christianson, D. W. (2009). *Biochemistry*, **48**, 121–131.
Stone, E. M., Glazer, E. S., Chantranupong, L., Cherukuri, P., Breece, R. M., Tierney, D. L., Curley, S. A., Iverson, B. L. & Georgiou, G. (2010). *ACS Chem. Biol.* **5**, 333–342.
Winn, M. D. *et al.* (2011). *Acta Cryst.* D**67**, 235–242.